AUTEX Research Journal, Vol. 18, No 4, December 2018, DOI: 10.1515/aut-2018-0019 © AUTEX

MEASUREMENT OF THE UNIFORMITY OF THERMALLY BONDED POINTS IN POLYPROPYLENE SPUNBONDED NON-WOVENS USING IMAGE PROCESSING AND ITS RELATIONSHIP WITH THEIR TENSILE PROPERTIES

Mina Emadi, Mohammad Ali Tavanaie*, Pedram Payvandy

Textile Engineering Department, Yazd University, Yazd, Iran
Corresponding author email: ma.tavanaie@yazd.ac.ir

Abstract:

This article aims at the image processing of surface uniformity and thermally bonded points uniformity in polypropylene spunbonded non-wovens. The investigated samples were at two different weights and three levels of non-uniformity. An image processing method based on the k-means clustering algorithm was applied to produce clustered images. The best clustering procedure was selected by using the lowest Davies-Bouldin index. The peak signal-to-noise ratio (PSNR) image quality evaluation method was used to choose the best binary image. Then, the non-woven surface uniformity was calculated using the quadrant method. The uniformity of thermally bonded points was calculated through an image processing method based on morphological operators. The relationships between the numerical outcomes and the empirical results of tensile tests were investigated. The results of image processing and tensile behavior showed that the surface uniformity and the uniformity of thermally bonded points have great impacts on tensile properties at the selected weights and non-uniformity levels. Thus, a sample with a higher level of uniformity and, consequently, more regular bonding points with further bonding percentage depicts the best tensile properties.

Keywords:

Thermally bonded non-wovens, Image processing, Bonding points, Tensile properties, k-means clustering

1. Introduction

Non-woven fabrics with two distinct areas, namely, fiber matrix and bonded points, demonstrate a special performance [1]. Determining the properties of non-wovens plays a substantial role in the extensive use of these fabrics for new applications. The spunbonding process is commonly used to produce non-woven fabrics [2]. Thermal bonding process has been widely used with different kinds of thermoplastic fibers. These include bicomponent and low-melting-point fibers. Among the various types of thermal bonding, the point bonding is the most widely used technique [3].

The image processing method has created a new branch in quality control and instrumentation; one can see that advanced imaging systems offered to the field for size assessment, calibration, transportation, production quality enhancement, inspection, grading, sorting, separation, and so on. Quality control issue is related to sampling of products, checkup of samples, and generalization of results to all products [4]. Determination of fabric properties and online controls such as control of web uniformity [5], defects [6], fiber diameter [7], and fiber orientation [8] are among the task that image processing systems can take over. This technology can function more accurately, quickly, and less erroneously than the human eye.

AS the term “uniformity” is defined as an index of variation in aspects such as fiber orientation, weight, thickness, density, and fiber diameter, the constancy or inconstancy of the measured values of these features in different locations of a non-woven web can be referred to as “uniformity” or “non-uniformity.” Many attempts have been made to find a reliable technique for determination of non-woven web uniformity. Some of them are offline measurements, in which the measurements cannot be performed while the machine is running, and some of them are online measurements, in which all the measurements and analyses can be performed while the machine is running, such as image base analysis.

There is a lot of research on the non-woven uniformity based on online measurements. Some researchers have used optical methods to evaluate changes in the basic weight. Veerabadran *et al*. (1996) examined a technique in which images and their optical densities were used to provide a uniformity index [9]. A similar trend was pursued by Boeckerman (1992). In his study, the non-woven fabrics were subjected to a transmitted light, a camera recorded the image intensity, and the sample optical density was related to the web weight [10]. In such techniques, the uniformity index is calculated by using the coefficient of variation (CV%) of the optical density, and measurements on various scales offer different indicators. Lien and Liu (2006) used optical intensity for online basic weight assessment, which, similar to other studies, had an inherent problem in that it relied on size [11]. In a study by Kallmes *et al*. (2000), an anisotropy analysis was done on planar stochastic structures and their relationship to other structural properties

was presented as a new index for quality control of such structures [12]. Cherkassky (1998) used the homogeneity and the inhomogeneity theory of irregular random fields to indicate deviations that would suggest degrees of non-uniformity [13]. Johansson (2000) recommended that Kurtosis can be used as a scale to gauge the non-uniformity of each quantifiable characteristic on a flat surface [14]. To determine the level of non-uniformity, wavelet analysis and LVQ neural network [15], Bayesian [16], and the generalized Gaussian density model [17] were used.

Another methodology for investigating the non-woven uniformity is the quadrant method based on image processing. The data received from the image processing method can be used to detect changes in the mass based on the alterations in the gray level. One of the studies to defeat the size reliance impediments in the coefficient of variation (CV%) analysis has been done by Pourdeyhimi and Kohel (2002) who defined a uniformity index by combined image processing and the quadrant method [18]. Amir Nasr *et al*. (2014) conducted a study to measure the uniformity of non-wovens with the known quadrant method [19]. Militky and Klicka (2007) chose a strategy to assess the non-woven uniformity in which rectangular arrays were used through the quadrant method [20]. They also obtained their information from the image processing method that measured the changes in mass based on the changes in the gray level using the coefficient of variation (CV%) and the one-way analysis of variance model.

The non-uniformity of non-woven fabrics affects their physical and esthetic properties [21]. Also, the non-uniformity of web influences permeability [22], tensile properties [23], and some other properties. One of the most important features of fabrics is their mechanical properties. Studying the tensile properties of non-woven fabrics is complicated because many structural parameters affect these properties. Tensile properties depend on three variables, including the mechanical properties of the constituent fibers [24]; the fiber orientation in the non-woven web [25], which mainly determines the anisotropy web; and the bonding points that make the connection between the fibers.

In the studies by Nohut *et al.* (2015) [26] and Taskan *et al.* (2015) [27], digital image analysis and artificial neural network were used to predict the weight, tensile strength, and elongation at the break values of the polypropylene non-woven fabrics with various weights.

There is a lot of literature on the analysis of the surface uniformity of non-wovens, but little information can be found for the prediction of tensile strength and elongation at peak points using digital image analysis. None of the abovementioned articles have made a reference to image processing of bonded points and the effect of their uniformity on the mechanical properties of non-woven fabrics. The bonded points are one of the main features of non-woven fabrics that may be unnoticed in visual quality controls. This structural feature affects the fabric tensile properties. However, strength is one of the extraneous features; thus, in all samples, only an insignificant factor such as a poor fiber or a weak link point can have a substantial effect on the fabric strength. In textile factories, strength measurement is usually done offline. Choosing this technique is effective because image processing systems can be applied to determine a uniformity index quickly and to do calculations fast and efficiently. This makes it significant to develop a technique for online applications. Applying the image processing method in online quality control is very useful and effective for factories that want to save time and money in this case. Noticing a variation in the quality of a product, one can find out the lack of uniformity. It leads to quick corrections in the production line and, thus, prevention of large amounts of shoddy products.

In this study, we evaluate the surface uniformity of the samples using the quadrant method. This method can be used to measure the overall uniformity of the samples in an image. A possible restriction in this study, which is related to the surface uniformity, is the use of binary images as the input images. The methodology of turning an image into a binary image can remove a lot of details. To overcome this limitation, the k-means clustering method is applied to produce binary images. In this method, certain degrees of intensity are assigned to certain layers (clusters). This algorithm is an effective way to convert images containing objects with different intensities to cluster images. Also, a proposed image processing method is used to evaluate the uniformity of thermally bonded points in non-woven fabrics. It is attempted to achieve an interaction between the tensile properties of non-woven fabrics and the non-woven dispersion indexes. To reach this end, the tensile properties of the non-woven samples are measured, and then the experimental data are compared with the obtained data from the image processing method.

2. Experimental

2.1. Material

The specimens were taken directly from a roll of a factory-made polypropylene thermally bonded non-woven fabric. Two sets of thermally bonded non-woven fabric were specially prepared by changing the degree of fiber dispersion, which led to different uniformity levels. In terms of fabric properties, the samples were tests and studied at two different weights (15 and 30 g/m^2) and three levels of uniformity (poor, medium, and good). The bonding temperature was 165°C, the nip pressure varied from 3 to 3.2 kg/cm^2 for two types of the samples, and production speed of the samples was 40 m/min. The samples were cut from different stances of the web and then weighted. The average weight and thickness (ASTM D-5729) of 10 specimens and the CV% for each fabric type are presented in Table 1.

2.2. Methods

2.2.1. Tensile test

The tensile properties of polypropylene non-woven fabrics were measured in a machine direction by an INSTRON tester in laboratory conditions (i.e., 20 ± 2°C and 50% humidity). The samples with a dimension of 25 cm × 10 cm were fixed to a

Table 1. The average weight, thickness, and CV% of polypropylene thermally-bonded non-woven

	S15-1	S15-2	S15-3	S30-1	S30-2	S30-3
Uniformity degree	Good	Medium	Poor	Good	Medium	Poor
Average weights (g/m²)	15.653	15.690	15.801	30.427	32.861	31.934
CV%	3.15	5.27	5.37	3.88	5.56	9.22
Average thickness (mm)	0.161	0.206	0.207	0.27	0.314	0.317
CV%	7.24	8.39	9.15	2.94	11.3	22.88

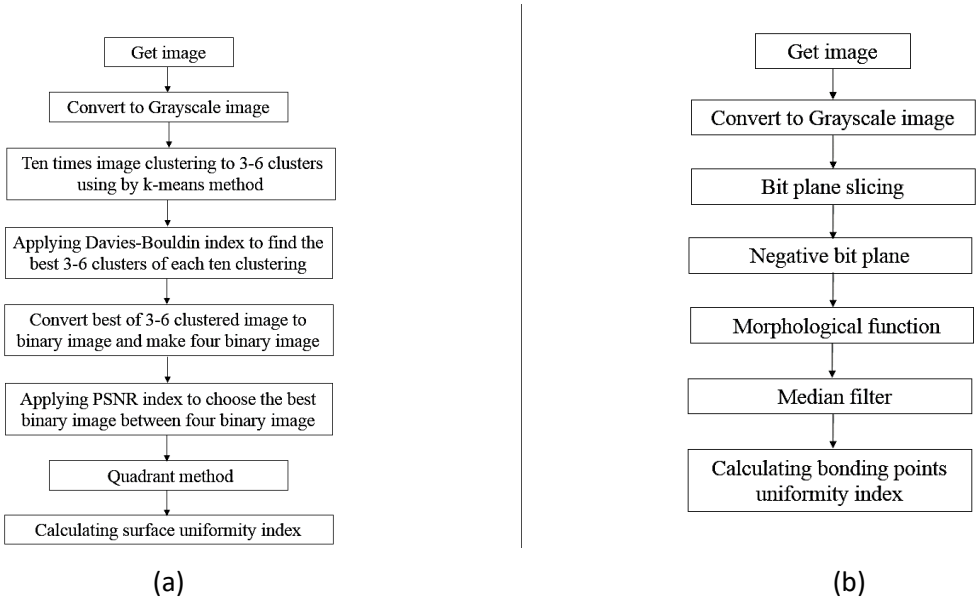

Figure 1. Flowchart of the image analysis algorithm: (a) surface uniformity image processing and (b) bonding points image processing

mechanical testing machine with a gage length of 150 mm (ASTM D-5034), while the grip size was considered as 5 cm on both sides of the test zone. The cross-head speed was constant and equal to 150 mm/s. For each sample, 10 specimens were used in the tensile test.

2.2.2. Image processing

2.2.2.1. Surface uniformity measurement

As shown in the flowchart of Figure 1(a), first, the color images of the samples were converted into grayscales and, afterward, a thresholding operation was done. In thresholding, a color image is converted into a black-and-white one. In this study, the k-means clustering method was applied to convert color images to black-and-white ones. The accuracy of extracting objects from a background image is increased by using this method. Clustering analysis is a branch of science that uses common data features to assign data into a predetermined number of clusters. One usage of this method is grouping points with the same intensity, which is practiced for classification and separation of objects from the background. The k-means clustering algorithm works with random cluster centers. So, clustering is influenced by the selected initial cluster centers, and the algorithm has no single response [28]. The noteworthy issue in this context is the problem of finding the optimal clustering, usually called “cluster validation”.

One of the clustering validity indices is Davies–Bouldin index. This index uses the similarity between two clusters (R_{ij}), which is defined based on the distribution of i-th cluster (S_i) and the lack of similarity between clusters i and j (d_{ij}). Davis–Bouldin index for clustering is defined as follows:

$$DB = \frac{1}{n_c}\sum_{i=1}^{n_c} R_i \tag{1}$$

where n_c is the number of clusters. R_i is defined as follows:

$$R_i = \max(R_{ij}) \, , i = 1 \ldots n_c \, , j = 1 \ldots n_c \, , i \neq j \tag{2}$$

In Equation (2), R_{ij} is the similarity between two clusters, which is defined as follows:

$$R_{ij} = \frac{S_i + S_J}{d_{ij}} \tag{3}$$

where d_{ij} and S_i are calculated using the following equation:

$$d_{ij} = d\left(v_i, v_j\right) \tag{4}$$

In Equation (4), d is the distance function, and v_i and v_j are i- and j-th cluster centers, respectively. So, d_{ij} will be the distance between i- and j-th cluster centers:

$$S_i = \frac{1}{||c_i||}\sum_{x \in c_i}^{\cdot} d(x, v_i) \tag{5}$$

In Equation (5), C_i is the number of data in the i-th cluster and v_i is the i-th cluster center. Davies–Bouldin index calculates the average of similarities between each cluster and the closest cluster to it. The most optimal clustering is achieved when the intracluster distance is of the lowest value and the distance between the clusters has the highest value. According to the definitions, it is understood that better clusters are produced with lower indices [29].

One of the important steps in making binary images by the clustering method is setting an appropriate number of clusters. As mentioned, an outcome is reasonable when the obtained binary image has negligible changes as compared to the original image. Therefore, to determine the appropriate number of clusters, the image-quality-determining methods should be used. The peak signal-to-noise ratio, often abbreviated as the PSNR index, is applied to assess the quality of a binary image using the k-means clustering method. The image is clustered using different numbers of clusters, and, then, the PSNR index is applied to the obtained binary image. An image with a higher index value is closer to the original one. This index is defined as follows:

$$MSE = \frac{1}{mn}\sum_{i=0}^{m-1}\sum_{j=0}^{n-1}(\mathrm{I}_{\mathrm{orginal}}(\mathrm{i},\mathrm{j}) - (\mathrm{I}_{\mathrm{bw}}(\mathrm{i},\mathrm{j}))^2 \quad (6)$$

$$\mathrm{PSNR} = 10\log\left(\frac{max\left(\mathrm{I}_{\mathrm{orginal}}\right)^2}{MSE}\right) \quad (7)$$

In these equations, m and n are image sizes, $I_{orginal}$ is the original image, I_{bw} is the binary image, and max ($I_{orginal}$) is the maximum value that image pixels can have.

The non-woven sample images are divided into 3–6 intensities or clusters. The k-means clustering method is performed 10 times for each image, and, then, the best one among 10 clusterings is selected using Davies–Bouldin index. After converting the best of 3–6 clustered images to a binary image and making four binary images, the PSNR index is applied to choose the best binary image among four images. After thresholding, the quadrant method is applied on each input image to assess the surface dispersion index of the non-woven samples (Figure 2).

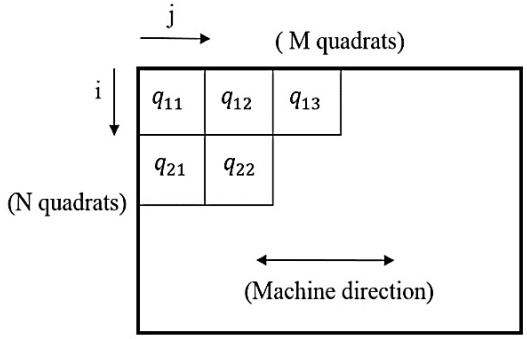

Figure 2. Average of white pixels after applying the quadrant method

In the quadrant method, the image is divided into squares and analyzed. This method is one of the techniques used in the environment to determine the characteristics of space [30]. The quadrant method in an image processing system allows defining a dispersion index that can be used to characterize the level of uniformity. The average number of white and gray pixels in a square (q_{ij}), the total average of white and gray pixels (Q) as the average value of the fiber fraction in surface, the standard deviation of them (SD), and their dispersion index (I_D) are calculated as follows:

$$Q = \frac{\sum_1^M \sum_1^N q_{ij}}{MN} \quad (8)$$

$$SD = \left(\frac{\sum_1^M \sum_1^N (q_{ij}-Q)^2}{MN}\right)^{1/2} \quad (9)$$

$$I_D = \frac{(SD)^2}{Q} \quad (10)$$

where M and N are the numbers of squares in length and width of the image. The surface dispersion index can be calculated using the average number of white pixels and used as a criterion to determine the surface uniformity of the non-woven fabrics.

2.2.2.2. Measuring the uniformity of thermally bonded points

The image processing technique associated with morphological operations is used to extract the bonding points and to analyze them in terms of uniformity. As shown in Figure 1(b), first, the color images are converted into grayscales. Second, bit plane slicing is applied to those grayscales to take out the best bit plane, which contains more visual information of the thermally bonded points. The highest-order planes contain a great deal of valuable visual data, while the lower-order planes include finer details of the image. So, a bit plane that provides more visual information of the thermally bonded points is selected. This plane is used as the selected binary image for further analysis. In the next step, the negative binary image of the bit plane is created and exposed to opening and closing functions as well as median filtering so as to remove undesirable details.

The two important operators of mathematical morphology are opening and closing functions, which are derived from the basic operators of erosion and dilation. These operators in computer vision and image processing serve as a basic function of morphological noise removal. The opening function eliminates tiny objects from the foreground of an image and places them in the background, while the closing function removes small holes in the foreground and changes the small islands of the background into the foreground. These techniques can also be used to find specific shapes in an image. Median filtering is a simple, intuitive, and easy-to-implement method of smoothing images, that is, reducing the amount of intensity variation between one pixel and the next. It is often used to reduce noise in images [31].

Eventually, by applying the above operations, the thermally bonded points are visible as white objects on a black background in the final binary image. The area of each bonding points, the percentage of the bonded area, and the average area of bonding points are calculated. Then, the dispersion index of the bonding points area (*Id*), which presents the amount of dispersion of the bonding points area, is calculated to evaluate the uniformity of the bonding points.

2.2.2.3. One-way analysis of variance

One-way analysis of variance is a technique that serves to compare means of three or more samples (using the F-distribution). In this study, one-way analysis of variance was used to investigate the effect of weight and the degree of uniformity on the surface dispersion index, bonding dispersion index, and the percentage of bonding points. The significance level α was equal to 0.05.

3. Results and discussion

A scanner with a resolution of 2,400 dpi was used to produce images of the non-woven samples. A black screen was placed behind the samples. All the image dimensions were limited to 10*15 cm^2. Three levels of the non-woven samples uniformity are shown in Figure 3.

3.1. Thresholding results

Thresholding is applied to images to evaluate the surface uniformity of sample using the image processing method. Typical thresholding is one of the most common methods that can be applied when the pixel intensity distribution of objects differs from that of the background. In other words, there can be an image containing a clear object in a dark background or vice versa. Binary images obtained through the typical thresholding method have been used as the initial images in some surface uniformity research [18, 19, 26, 27]; however, the background in the non-woven sample images with different intensities is not clear and distinct. Thus, the process of turning them into binary images through typical thresholding can destroy a lot of details. Something that can overcome this limitation is the k-means clustering method. The k-means clustering method has been used to study the thresholds of images. Dehghan and et al. showed in their studies that the clustering method presented the best results compared with the typical thresholding [32]. Also, Lin et al. [33] and Srinivas et al. [34] found the k-means algorithm as a suitable method to extract the object from the background in the images.

The non-woven sample images were divided into 3–6 intensities or clusters and, for each image, the k-means clustering method was applied 10 times (Table 2). Then, the best of the 10 clusters was selected using the lowest Davies–Bouldin index. After converting the best of 3–6 clustered images to binary ones and making four binary images, 4 clusters were selected as the best number of clusters with the highest PSNR indices. Figures 5 and 6 present the image clustering results in 4 clusters, the Davies–Bouldin and PSNR values for each sample. The binary image obtained from the clustering method is selected for future analysis.

3.2. Surface uniformity analysis

The non-woven samples were cut into the sizes given in Table 3 and then were weighed. The weight dispersion index values were calculated to verify the data obtained from the image processing method (quadrant method). Two dispersion index values were obtained from the image processing and weighing methods. The corresponding correlation coefficients are presented in Table 3. As it can be seen, the correlation coefficient values for all the samples are greater than 0.95. Generally, a correlation coefficient shows the relationship between two variables. So, coefficient values greater than 0.95 show a strong and positive relationship between the image processing and the weighing methods. Figure 7 provides the results of the image processing and the weighting methods and their proportions.

The results of the image processing method were well correlated with the weighing results. They were also compatible with the degree of sample visual uniformity (Figure 3). Therefore, it is realized that, in each group with the same weighted average, the lower degree of sample surface uniformity causes the higher dispersion index. It seems that the quadrant method is

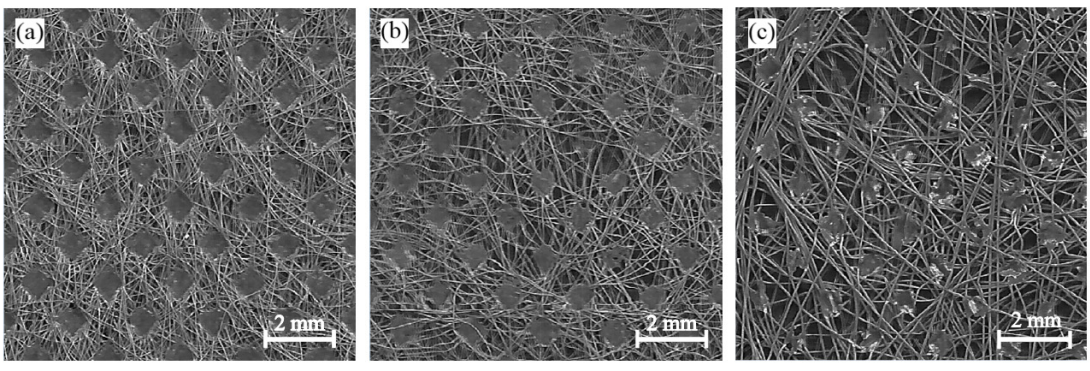

Figure 3. Three levels of 30-g/m^2 samples uniformity: (a) sample with the highest uniformity, (b) sample with the medium uniformity, (c) sample with the lowest uniformity

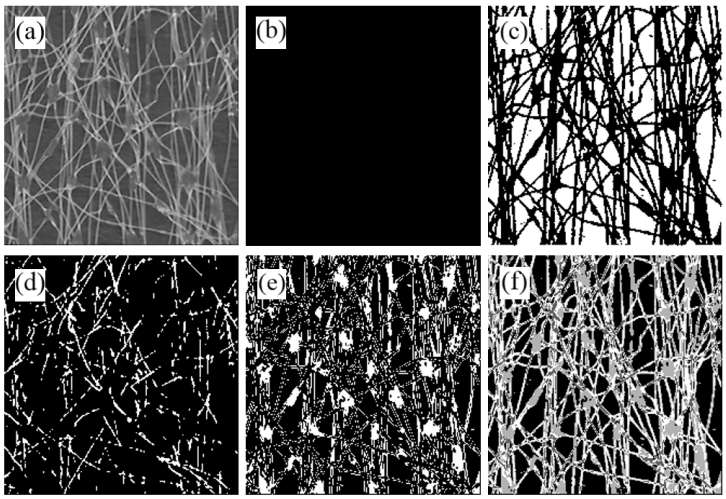

Figure 4. Sample S15-3 after applying the k-means clustering method: (a) original image, (b) the first layer, (c) the second layer, (d) the third layer (e) the fourth layer, and (f) collecting all the layers together

Table 2. The PSNR and Davies–Bouldin index values for polypropylene non-woven samples

Sample		k = 3	k = 4	k = 5	k = 6
S15-1	**PSNR**	6.5872	6.6296	6.6567	6.5165
	DB	0.4598	0.4153	0.4220	0.3981
S15-2	**PSNR**	6.7561	6.9211	6.8672	6.8629
	DB	0.4414	0.4330	0.4307	0.3962
S15-3	**PSNR**	7.2208	7.2438	7.1428	7.2793
	DB	0.4062	0.4422	0.4134	0.4051
S30-1	**PSNR**	8.2985	8.3098	8.3025	8.2904
	DB	0.4540	0.4269	0.4464	0.4090
S30-2	**PSNR**	8.1041	8.1269	8.1587	8.1332
	DB	0.4444	0.4422	0.4474	0.4103
S30-3	**PSNR**	9.0382	9.1187	9.0969	9.1413
	DB	0.4380	0.4359	0.4398	0.4312

an appropriate method to determine the surface uniformity of the non-woven fabrics. Similar results were presented in the Nohut *et al*. [26] and Taskan *et al.* [27] studies. So, the non-woven fabrics with the different levels of uniformity can be well recognized by this method.

3.3. Bonding uniformity analysis

The color images were converted into grayscales, then the bit-plane slicing was done to them to extract and analyze the uniformity of the thermally bonded points. Figure 8(a) is an 8-bit grayscale image, and Figure 8(b) to 8(i) is its 1-bit planes. Each bit plane is a binary image.

As shown in Figure 8(g), the 6th bit plane, compared to the other bit planes, reveals the best information about the thermally bonded points. So, it could be used as a selected binary image for subsequent analyses. After that, the morphological operations and the median filtering were done to clear the thermally bonded points and remove irrelevant details. Figure 9 shows the sequence of operations applied to the images. The final image is a binary image in which the thermally bonded points are visible as white objects on a black background. The measured values of the bonding average area, the bonding dispersion indices, and their percentages by the image processing method are presented in Table 4. Also, Figure 10 presents the corresponding changing trends with which to assess the influence of the surface uniformity on the bonding points uniformity.

A weight gain of 15–30 g in the two samples S30-1 and S15-1 increased the quantity of fibers per area unit and the web density. It can be argued that by increasing the web covering, the bonding calendar affected more fibers, and,

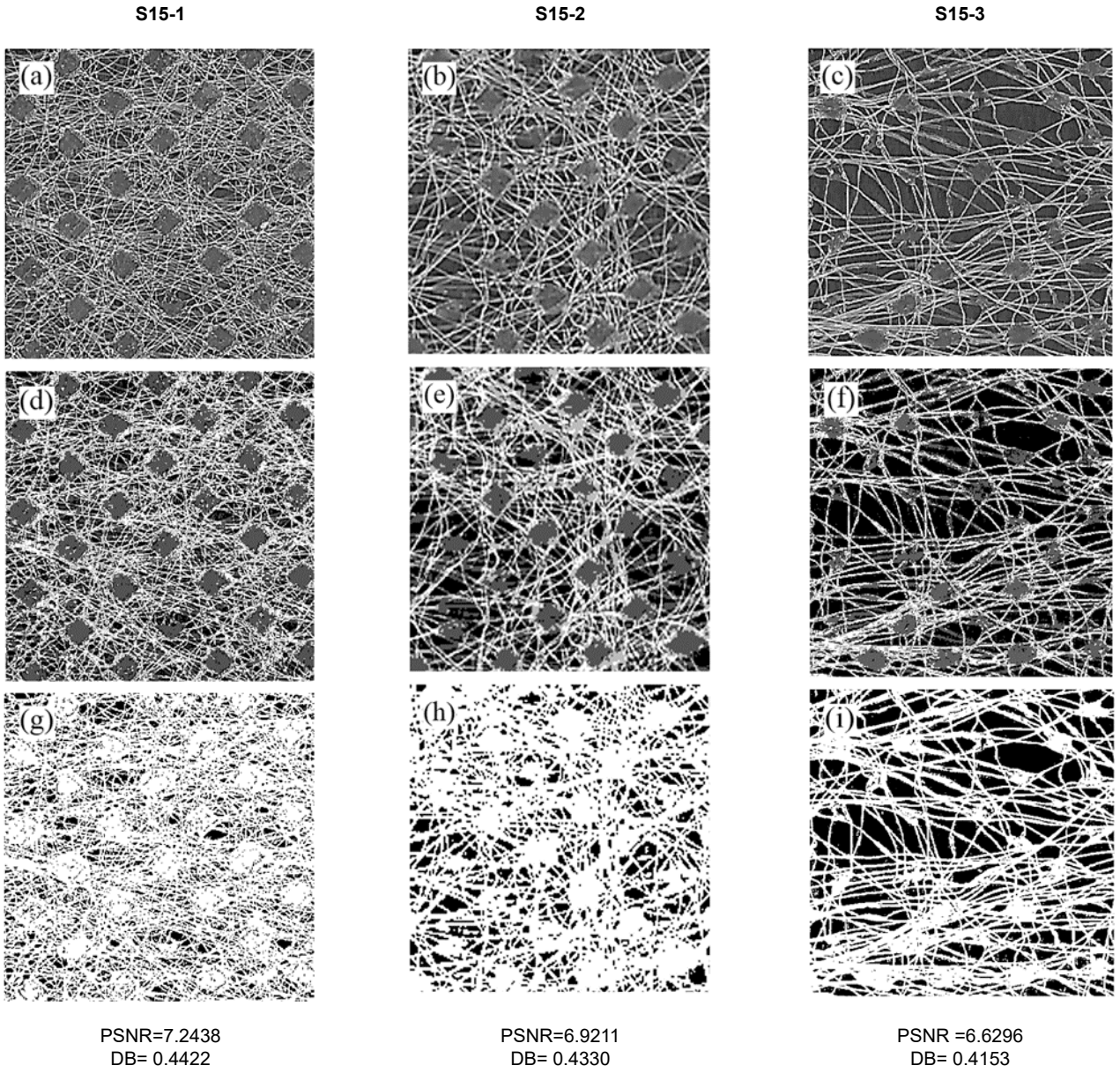

Figure 5. (a), (b), and (c) the grayscale images of 15-g/cm^2 sample; (d), (e), and (f) the clustered images obtained by the k-means clustering method with 10-time repetitions and 4 clusters; (g), (h), and (i) the binary images of (d), (e), and (f)

therefore, every bonded point was closer to the bonding pattern. The values for the bonding average area, presented in Table 4, are suggestive of this matter. However, in a group with the same weighted average and the different degrees of uniformity, a decrease in the surface uniformity led to a reduction in the bonding average area. In other words, with a decrease in the surface uniformity, the possibility of existing empty pores in some areas of the web is increased. So, when a non-woven web is placed under a thermal bonding calendar, some of the calendar bumps occur in the empty pores. This prevents the formation of bonding points, and even if they are formed, they will be sketchy. It also reduces the bonding average area and the bonding percentage, which, in consequence, affects the relevant statistical indicators. All this leads to the reduced possibility of forming uniform bonding points. What occurs in this regard is confirmed by the presented dispersion index. To sum up, the lower bonding uniformity, the lower surface uniformity, thus, the higher bonding dispersion index.

3.4. One-way analysis of variance results

Table 5 presents the results of the one-way analysis of variance. The significance value for each dependent parameter is 0.000, which indicates a significant difference in the mean of each dependent parameter.

3.5. Tensile testing results

Strength and elongation in break tests were performed on the samples to study the effects of surface uniformity, bonding uniformity, and their percentage on the mechanical properties. Figure 11 shows the stress–strain curves at the maximum stress, and Table 6 presents the maximum stress, the strain at the maximum stress, and the initial modulus values. Table 7 presents the results of the one-way analysis of variance for tensile properties. The significance value for each dependent parameter is 0.000, which indicates a significant difference in the mean of each dependent parameter.

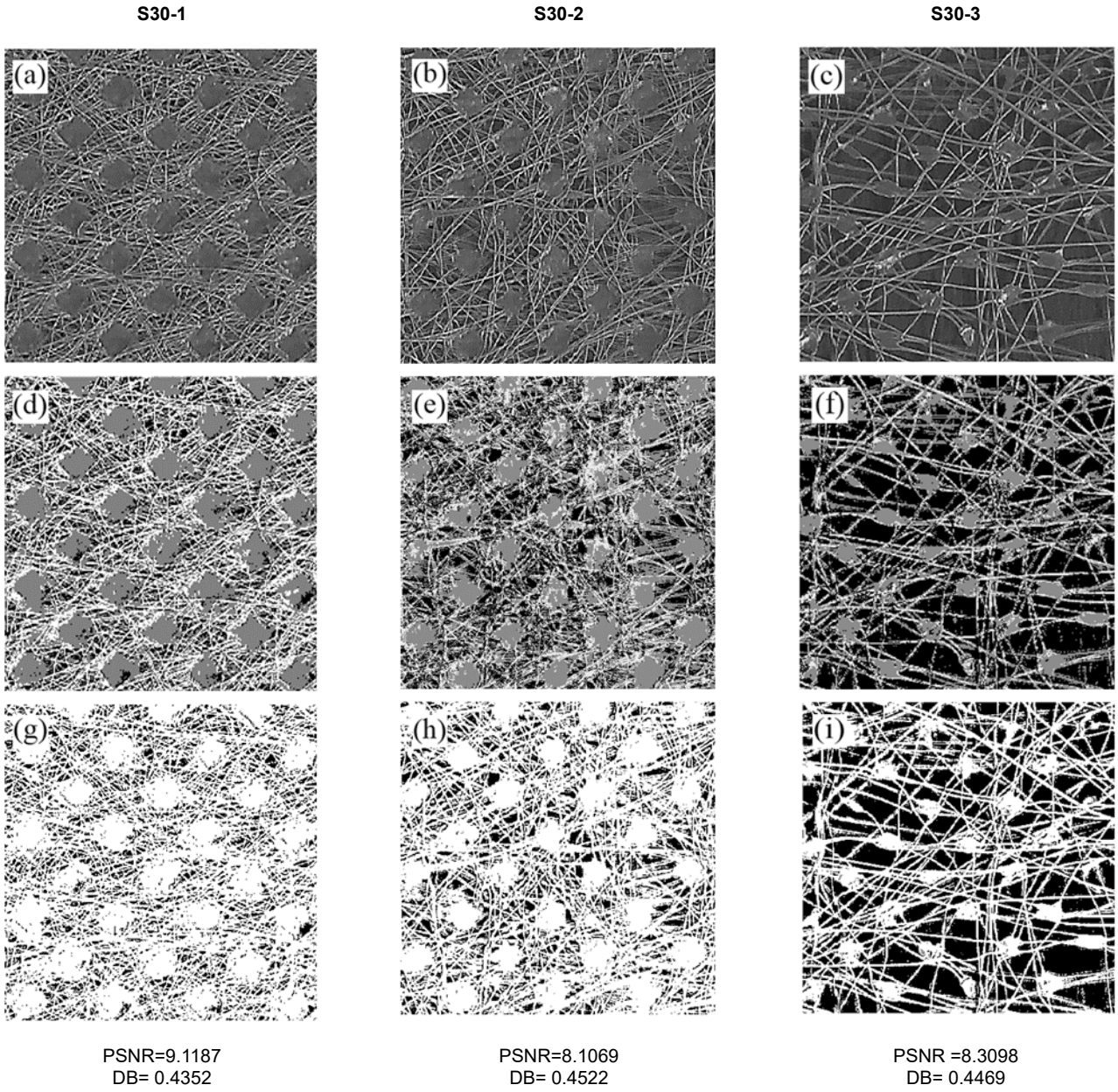

Figure 6. (a), (b), and (c) the grayscale images of 30-g/cm^2 sample; (d), (e), and (f) the clustered images obtained by the k-means clustering method with 10-time repetitions and 4 clusters; (g), (h), and (i) the binary images of (d), (e), and (f)

As shown in Table 6 and Figure 11, in each group of samples with the same weighted average, a sample with the further surface uniformity, the regular bonding points, and a higher percentage of bonding demonstrates higher maximum stress and strain and a greater initial modulus as compared with the other samples. So, the lower degree of surface uniformity presents the lower maximum stress, the strain at maximum stress, and the initial modulus. By comparing the presented coefficients of variation (CV%) for stress and strain, it emerges that for a sample with more weight, the CV% value is lower. It can be claimed that with an increase in the weight, the possibility of the surface uniformity, and the uniformity of thermally bonded points is increased, and, consequently, the dispersion of tensile properties is reduced. On the other hand, in each group of samples with the same weighted average, it seems obvious for a sample with a medium surface uniformity to have a higher CV% value than a sample with the highest surface uniformity. However, a sample with the lowest surface uniformity has a lower CV% value than a sample with a medium uniformity. It may be because these samples have an extreme non-uniformity in their structures and are broken fast in a certain period of time, which makes the CV% values of these samples lower than those of the samples with a medium uniformity. Samples with a poor surface uniformity have a brittle mode and a very low elongation at break. For instance, for sample S15-3, the strain is about 15%, and for sample S30-3, it is less than 10%. For this reason, these samples are not suitable for commercial use. The important issue is the downtrend of stress and strain in each weighting group, which is consistent well with the degree of samples surface uniformity.

Figure 12 shows the interaction between the image processing data and the experimental results obtained from the tensile test for two groups with the same weighted average. It can be seen that in each weighting group, the surface dispersion index and

Table 3. Dispersion indices obtained from the two methods of image processing and weighing and their corresponding correlation coefficients

Samples	Size of squares (cm²)	Image processing dispersion index (IPDI)	Weight dispersion index (WDI)	R^2 (Correlation coefficient)
S15-1	5 × 5	0.0134×10^{-2}	0.0188	0.9704
	2.5 × 2.5	0.1646×10^{-2}	0.0592	
	1.25 × 1.25	0.3041×10^{-2}	0.1388	
S15-2	5 × 5	0.3467×10^{-2}	0.0614	0.9639
	2.5 × 2.5	0.4406×10^{-2}	0.1055	
	1.25 × 1.25	0.5682×10^{-2}	0.2882	
S15-3	5 × 5	0.2075×10^{-2}	0.1333	0.9957
	2.5 × 2.5	0.3313×10^{-2}	0.1922	
	1.25 × 1.25	0.7182×10^{-2}	0.3242	
S30-1	5 × 5	0.0053×10^{-2}	0.1291	0.9972
	2.5 × 2.5	0.0128×10^{-2}	0.2036	
	1.25 × 1.25	0.0215×10^{-2}	0.5788	
S30-2	5 × 5	0.0378×10^{-2}	0.7867	0.9595
	2.5 × 2.5	0.0532×10^{-2}	1.0190	
	1.25 × 1.25	0.0712×10^{-2}	1.6172	
S30-3	5 × 5	0.1757×10^{-2}	1.0112	0.9973
	2.5 × 2.5	0.2982×10^{-2}	1.6223	
	1.25 × 1.25	0.4159×10^{-2}	2.3254	

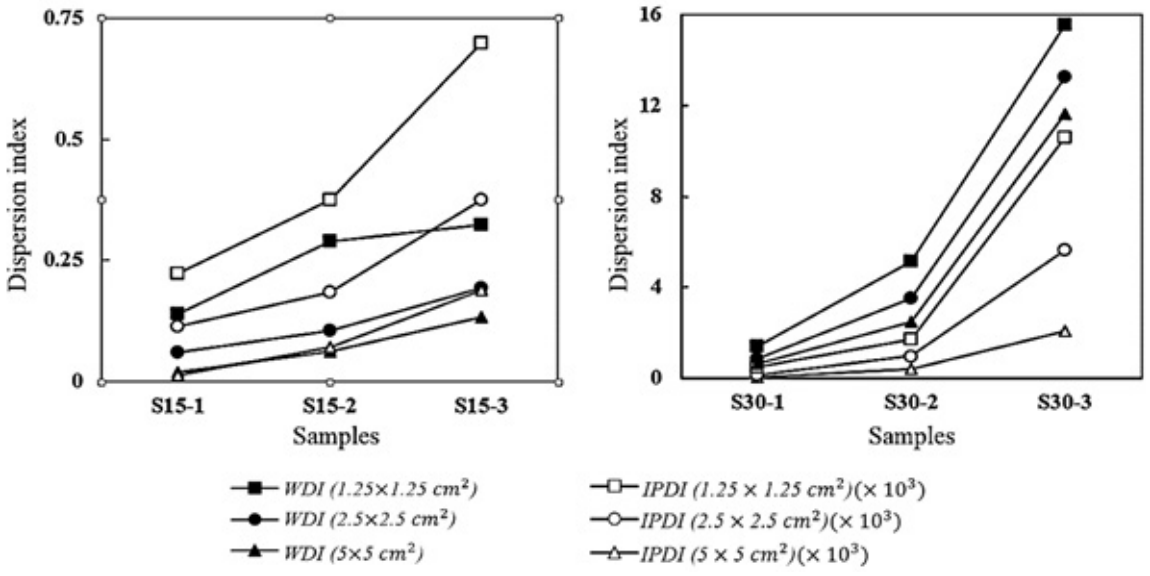

Figure 7. Surface dispersion index curves obtained from the image processing and the weighing methods

Table 4. The parameters of thermally bonded points obtained from the image processing method

	S15-1	S15-2	S15-3	S30-1	S30-2	S30-3
Bonding average area (mm²)	0.3023	0.2424	0.2190	0.3642	0.3403	0.1475
Bonding dispersion index	1.2456	3.0454	7.7126	1.2626	2.1874	4.7308
Bonding percentage (%)	13.0093	10.9609	8.8300	18.4674	15.9942	7.0715

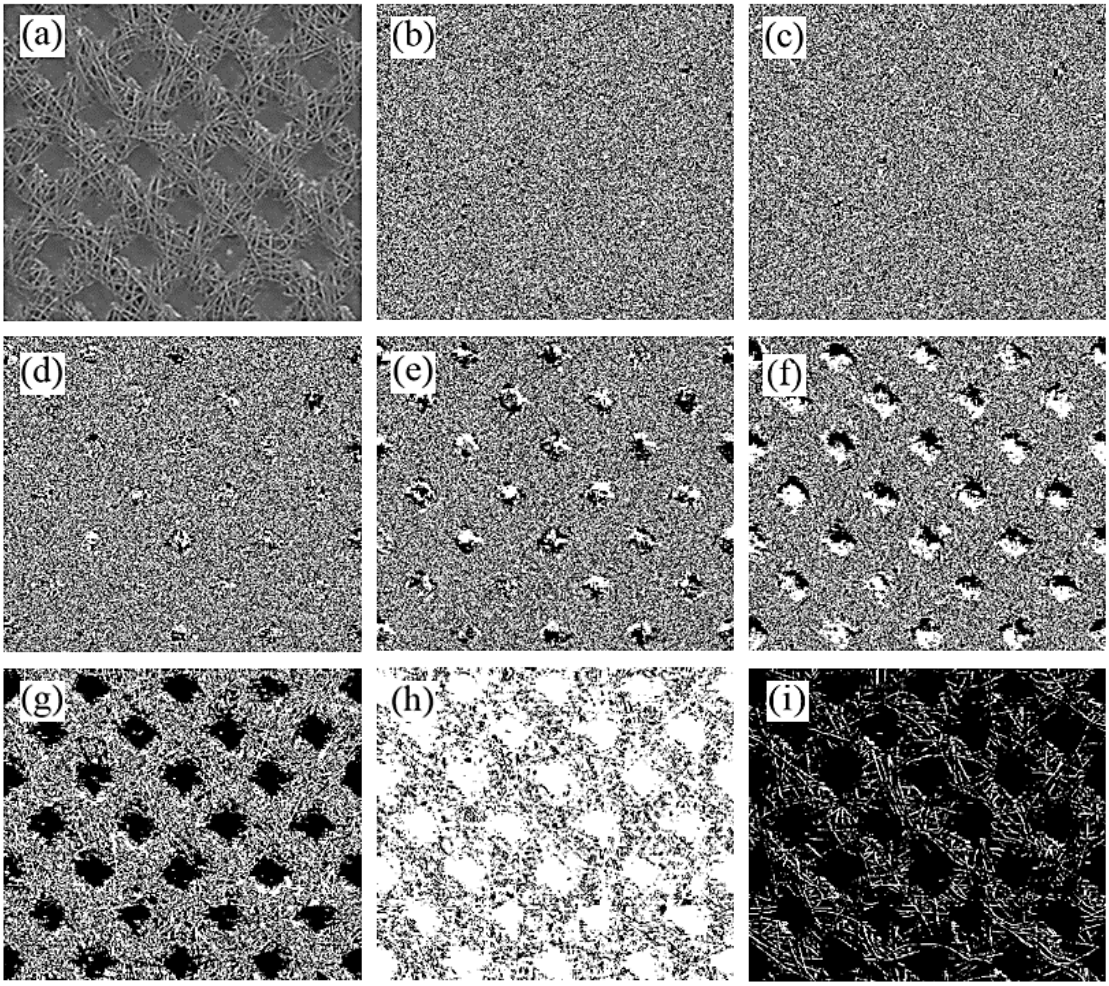

Figure 8. (a) 8-bit grayscale image, (b) to (i) are 1- to 8-bit planes, 1-bit plane corresponding to the least important bit

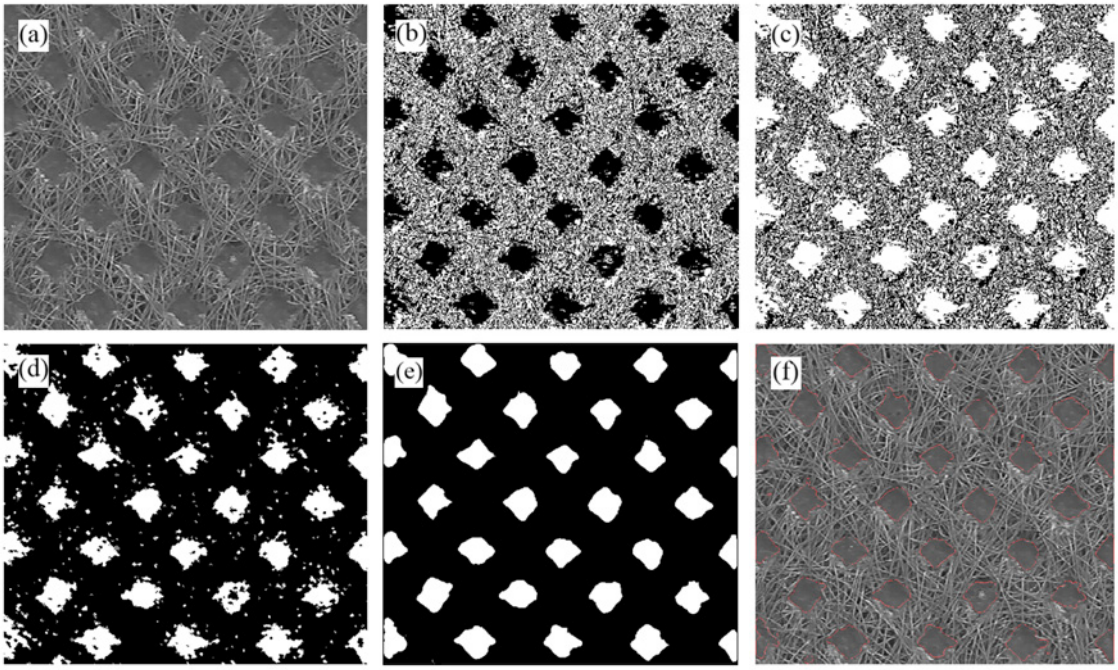

Figure 9. The sequence of operations to extract the bonding points: (a) the grayscale image, (b) the 6th bit plane, (c) the 6th bit plane negative, (d) after applying morphological operations, (e) after applying median filter, and (f) outline bonding points in the original image

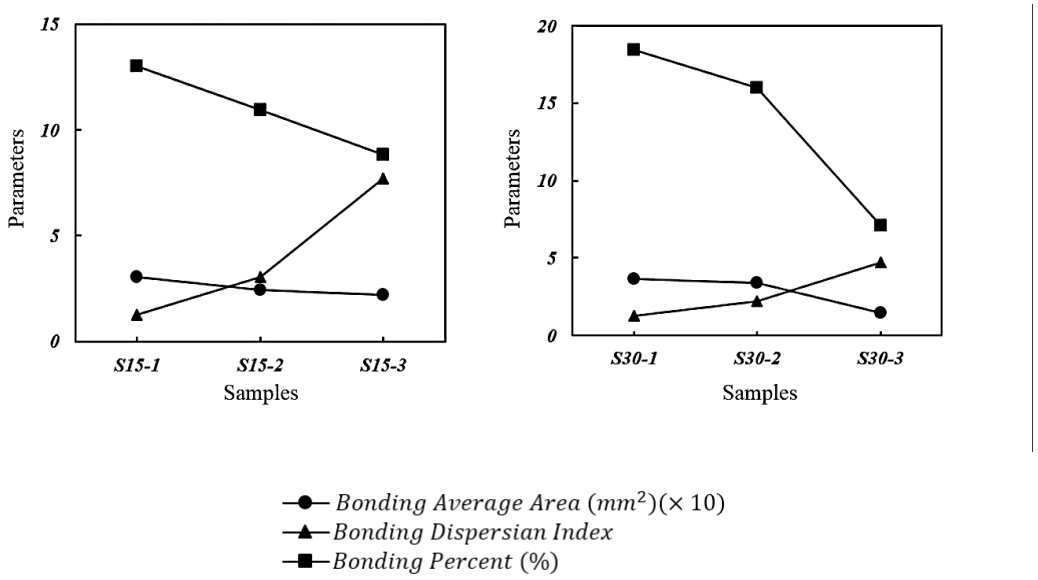

Figure 10. The changing trends of the parameters of thermally bonded points (the bonding average area, the bonding dispersion index, and the bonding percentage)

Table 5. One-way analysis of variance results for weight and image processing

	F (15 g/m²)	F (30 g/m²)
Weight dispersion index (5 × 5 cm²)	7,763.83	9,586.584
Weight dispersion index (2.5 × 2.5 cm²)	7,016.295	9,239.658
Weight dispersion index (1.25 × 1.25 cm²)	9,987.256	10,259.658
Image processing dispersion index (5 × 5 cm²)	65.656	1,107.697
Image processing dispersion index (2.5 × 2.5 cm²)	55.793	396.994
Image processing dispersion index (1.25 × 1.25 cm²)	283.575	1,080.663
Bonding dispersion index	187.660	264.091
Bonding percent	71.188	783.068

the bonding dispersion index are increased, but the percentage of bonding, the maximum stress, and the strain at the maximum stress point are decreased in pace with a decrease in the degree of the surface uniformity. A sample that presents poor results and the worst structural and bonding properties in the image processing method will have the worst tensile properties. This suggests that with the less surface uniformity or the worse bonding structure, the tensile properties are lower.

4. Conclusion

The key issue to improved tensile properties is the production of a web with a high bonded uniformity, which results from the surface uniformity. In the absence of an economical online method for measuring the uniformity of non-wovens, this article has aimed at whether a digital image processing system can be used to measure surface and bonding uniformity and estimate tensile properties. We have studied the association between web weight and image processing output using the quadrant method (i.e., a method to evaluate surface uniformity). There is a good linear correlation found in this regard. Indeed, a correlation coefficient of more than 0.95 is observed for all the samples between fiber weight and image processing output (surface uniformity). The results indicate that a scanner can be used to measure the surface uniformity for polypropylene non-wovens at web weights ranging from 15 to 30 g/m^2. In the image processing of the bonding points uniformity, it was observed that a sample with a higher surface uniformity has a lower bonding dispersion index, a higher bonding average area, and a higher bonded zones percentage. The maximum stress, the strain at the maximum stress, and the initial modulus are decreased by a decrease in the degree of surface uniformity. In the stress and strain measurements, it was found that for a sample with more weight, the CV% value is lower, and a sample with a medium surface uniformity has a higher CV% value than a sample with the highest surface uniformity. However, a sample with the lowest surface uniformity has a lower CV% value than a sample with a medium uniformity.

A sample that presents poor results and proves to have the worst structural and bonding properties in the image processing method will have the worst tensile properties. This indicates

Table 6. The maximum stress, the strain at the maximum stress, and the initial modulus results

		S15-1	S15-2	S15-3	S30-1	S30-2	S30-3
Maximum stress (MPa)	Mean	2.2066	1.3711	1.0748	2.3421	1.3529	0.8773
	CV%	4.840	8.919	8.61	5.667	12.2201	12.249
Strain at maximum stress (%)	Mean	36.0281	35.9719	13.639	154.809	48.196	6.649
	CV%	20.894	36.319	22.112	15.458	29.169	17.319
Initial modulus		0.3952	0.3368	0.2967	0.4886	0.3158	0.2421

Table 7. The one-way analysis of variance results for tensile properties

	F (15 g/m^2)	F (30 g/m^2)
Maximum stress (MPa)	31.701	227.088
Strain at maximum stress (%)	361.329	296.431

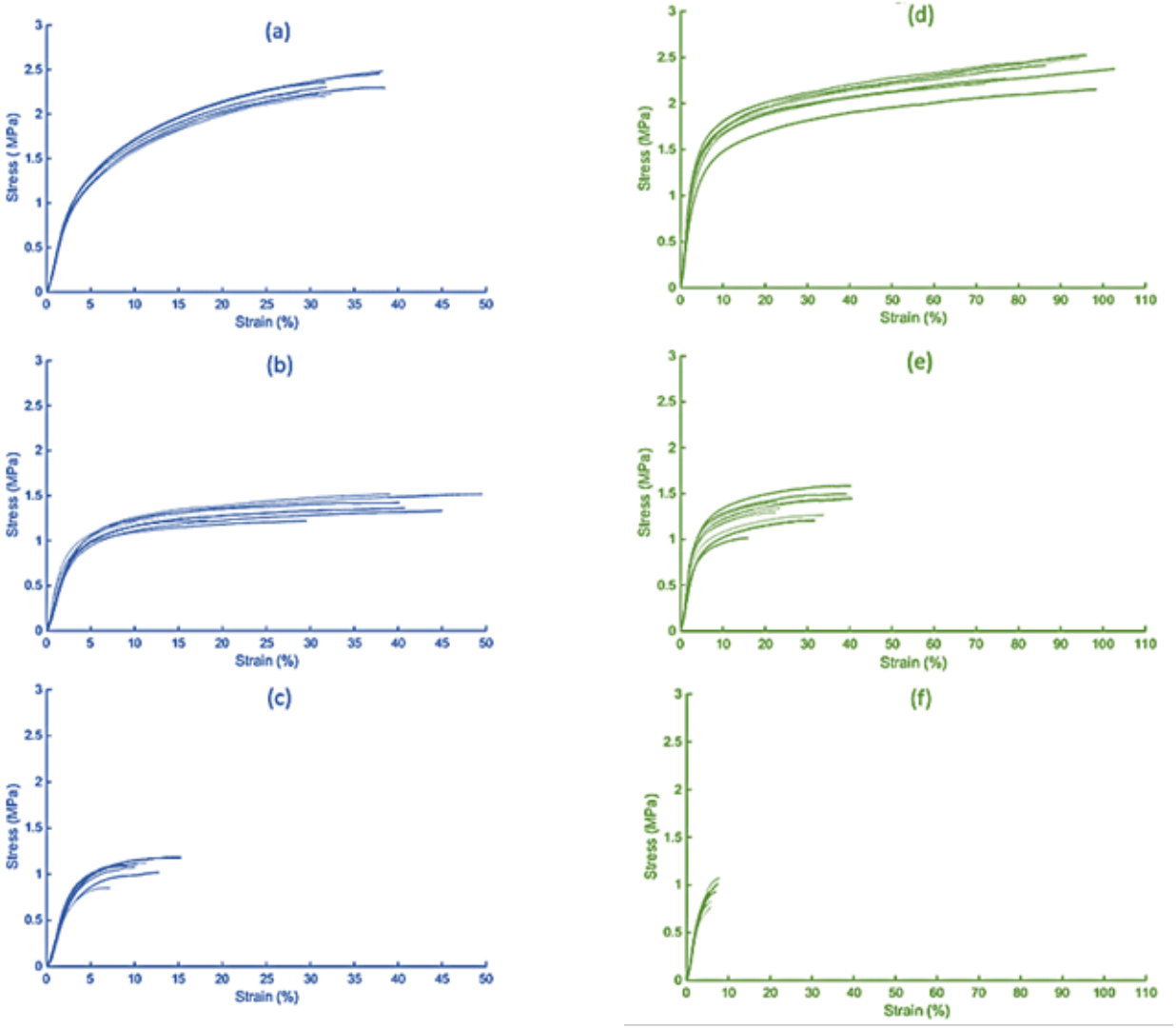

Figure 11. The stress–strain curves of the polypropylene spunbonded non-woven: (a), (b), and (c) samples S15-1, S15-2, and S15-3 (blue) and (d), (e), and (f) samples S30-1, S30-2, and S30-3 (green), respectively.

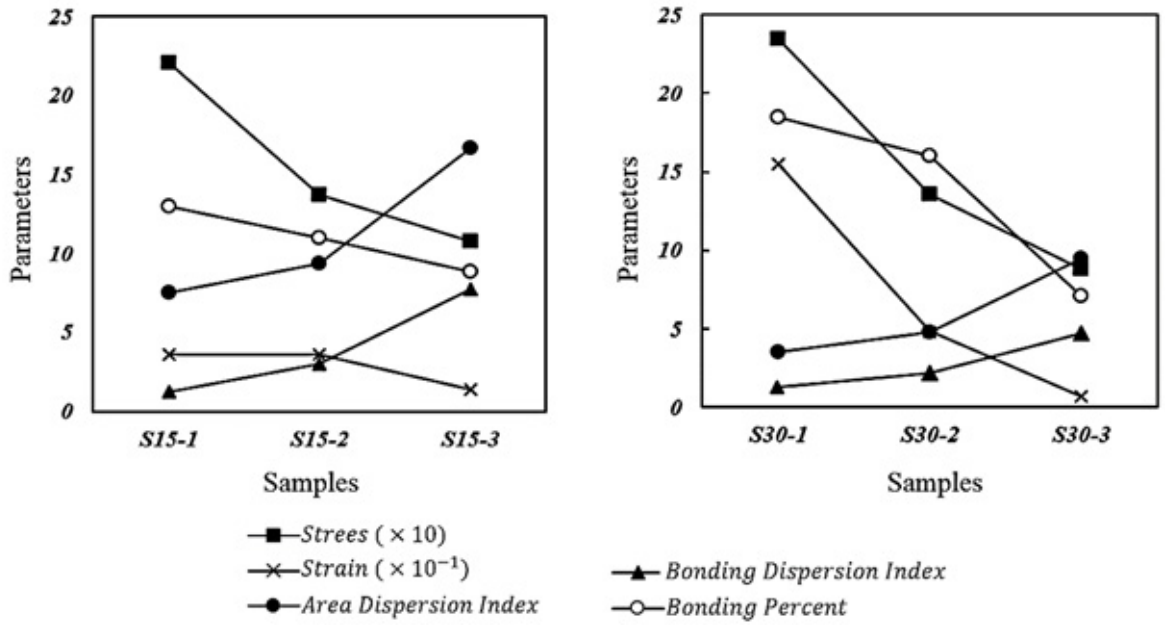

Figure 12. The image processing and the tensile testing parameters and also the interaction between them

that the less surface uniformity or the worse bonding structure has the lower tensile properties. This is a significant point to consider when adjusting a technique for an online application. By changing the product, the lack of uniformity, if any, is recognized and corrections are made on the production line quickly. This is how large production of shoddy products will be prevented. Applying the image processing method to online quality control is very useful and effective for factories that like to save time and money on quality control.

References

[1] *E. Demirci, "Mechanical behaviour of thermally bonded bicomponent fibre nonwovens: experimental analysis and numerical modelling," © Emrah Demirci, 2011.*

[2] *H. Lim, "A review of spunbond process," Journal of Textile and Apparel, Technology and Management, vol. 6, 2010.*

[3] *R. K. Dharmadhikary, T. Gilmore, H. Davis, and S. Batra, "Thermal bonding of nonwoven fabrics," Textile Progress, vol. 26, pp. 1-37, 1995.*

[4] *K. Yıldız, A. Buldu, and M. Demetgul, "A thermal-based defect classification method in textile fabrics with K-nearest neighbor algorithm," Journal of Industrial Textiles, vol. 45, pp. 780-795, 2016.*

[5] *G. Sun, X. Sun, and X. Wang, "Study on uniformity of a melt-blown fibrous web based on an image analysis technique," e-Polymers, vol. 17, pp. 211-214, 2017.*

[6] *K. Yildiz, A. Buldu, M. Demetgul, and Z. Yildiz, "A novel thermal-based fabric defect detection technique," The Journal of The Textile Institute, vol. 106, pp. 275-283, 2015.*

[7] *S. Li, H. Yi, and S. Shang, "Measurement of diameter and scale of cashmere fibers by computer image analysis," Journal of Fiber Bioengineering and Informatics, vol. 5, pp. 95-103, 2012.*

[8] *H. Merbold, D. Maas, and J. van Mechelen, "Multiparameter sensing of paper sheets using terahertz time-domain spectroscopy: Caliper, fiber orientation, moisture, and the role of spatial inhomogeneity," in SENSORS, 2016 IEEE, 2016, pp. 1-3.*

[9] *R. Veerabadran, H. Davis, S. Batra, and A. Bullerwell, "Devices for On-Line Assessment of Nonwovens' Basis Weights and Structures," Textile research journal, vol. 66, pp. 257-264, 1996.*

[10] *P. A. Boeckerman, "Meeting the special requirements for on-line basis weight measurement of lightweight nonwoven fabrics," Tappi journal, vol. 75, pp. 166-172, 1992.*

[11] *H.-C. Lien and C.-H. Liu, "A method of inspecting non-woven basis weight using the exponential law of absorption and image processing," Textile research journal, vol. 76, pp. 547-558, 2006.*

[12] *A. Kallmes, J. Scharcanski, and C. Dodson, "UNIFORMITY & ANISOTROPY IN NONWOVEN FIBROUS MATERIALS," in TAPPI NONWOVENS CONFERENCE, 2000, pp. 47.0-47.0.*

[13] *A. Cherkassky, "Analysis and simulation of nonwoven irregularity and nonhomogeneity," Textile research journal, vol. 68, pp. 242-253, 1998.*

[14] *J.-O. Johansson, "Measuring homogeneity of planar point-patterns by using kurtosis," Pattern Recognition Letters, vol. 21, pp. 1149-1156, 2000.*

[15] *J. Liu, B. Zuo, X. Zeng, P. Vroman, and B. Rabenasolo, "Nonwoven uniformity identification using wavelet texture analysis and LVQ neural network," Expert Systems with Applications, vol. 37, pp. 2241-2246, 2010.*

[16] *J. Liu, B. Zuo, X. Zeng, P. Vroman, and B. Rabenasolo, "Wavelet energy signatures and robust Bayesian neural network for visual quality recognition of nonwovens," Expert Systems with Applications, vol. 38, pp. 8497-8508, 2011.*

[17] *J. Liu, B. Zuo, X. Zeng, P. Vroman, and B. Rabenasolo, "Visual quality recognition of nonwovens using generalized Gaussian density model and robust Bayesian neural network," Neurocomputing, vol. 74, pp. 2813-2823, 2011.*

[18] *B. Pourdeyhimi and L. Kohel, "Area-based strategy for determining web uniformity," Textile research journal, vol. 72, pp. 1065-1072, 2002.*

[19] E. Amirnasr, E. Shim, B.-Y. Yeom, and B. Pourdeyhimi, "Basis weight uniformity analysis in nonwovens," The Journal of The Textile Institute, vol. 105, pp. 444-453, 2014.

[20] J. Militký and V. Klicka, "Nonwovens uniformity spatial characterization," Journal of Information and Computing Science, vol. 2, pp. 85-92, 2007.

[21] C. Ericson and J. Baxter, "Spunbonded Nonwoven Fabric Studies I: Characterization of Filament Arrangement in the Web," Textile Research Journal, vol. 43, pp. 371-378, 1973.

[22] M. Mohammadi and P. Banks-Lee, "Air permeability of multilayered nonwoven fabrics: Comparison of experimental and theoretical results," Textile Research Journal, vol. 72, pp. 613-617, 2002.

[23] X. Hou, M. Acar, and V. V. Silberschmidt, "Tensile behavior of low density thermally bonded nonwoven material," Journal of Engineered Fibers and Fabrics, vol. 4, pp. 26-33, 2009.

[24] C.-W. Lou, C.-T. Hsieh, S.-W. Lin, Y.-J. Pan, S.-Y. Huang, and J.-H. Lin, "Highly Resilient Polyester/Low Melting Point Polyester Protective Nonwoven Fabrics: Manufacturing Techniques and Mechanical Properties," DEStech Transactions on Engineering and Technology Research, 2017.

[25] O. Stolyarov and S. Ershov, "Characterization of change in polypropylene spunbond nonwoven fabric fiber orientation during deformation based on image analysis and Fourier transforms," The Journal of Strain Analysis for Engineering Design, p. 0309324717727235, 2017.

[26] S. Nohut and T. Arici, "Estimation of Areal Weight, Grab Tensile Strength, and Elongation at Break of PP Spunbond Nonwovens using Digital Image Analysis and Artificial Neural Networks," Journal of Engineered Fabrics & Fibers (JEFF), vol. 10, 2015.

[27] M. Taşcan and S. Nohut, "Nondestructive prediction of areal weight, grab tensile strength and elongation at break of polypropylene (PP) spunbond nonwoven fabrics using digital image analysis," Journal of Textile & Apparel/Tekstil ve Konfeksiyon, vol. 25, 2015.

[28] J. MacQueen, "Some methods for classification and analysis of multivariate observations," in Proceedings of the Fifth Berkeley Symposium on Mathematical Statistics and Probability, Volume 1: Statistics, Berkeley, Calif., 1967, pp. 281-297.

[29] D. L. Davies and D. W. Bouldin, "A cluster separation measure," IEEE transactions on pattern analysis and machine intelligence, pp. 224-227, 1979.

[30] P. Greig-Smith, Quantitative plant ecology vol. 9: Univ of California Press, 1983.

[31] R. C. Gonzalez and R. E. Woods, "Digital image processing," Nueva Jersey, 2008.

[32] N. Dehghan, M. A. Tavanaie, and P. Payvandy, "Morphology study of nanofibers produced by extraction from polymer blend fibers using image processing," Korean Journal of Chemical Engineering, vol. 32, pp. 1928-1937, 2015.

[33] W.-T. Lin, C.-H. Lin, T.-H. Wu, and Y.-K. Chan, "Image segmentation using the k-means algorithm for texture features," World Academy of Science, Engineering and Technology, vol. 65, pp. 612-615, 2010.

[34] K. Srinivas and D. V. Srikanth, "A Scientific Approach for Segmentation and Clustering Technique of Improved K-Means and Neural Networks," International Journal of Advanced Research in Computer Science and Software Engineering, vol. 2, 2012.